COBEM 2021 26th International Congress of Mechanical Engineering
ABCM Associação Brasileira de Engenharia e Ciências Mecânicas
November 22-26, 2021, Virtual Congress, Brazil

COB-2021-826
AEROELASTIC MODEL IDENTIFICATION OF AN AIRFOIL WITH THE USE OF ORTHOGONAL FUNCTIONS

Pedro Fernandes R. Bonnas[1]
Tobias Souza Morais[2]
Faculty of Mechanical Engineering, Federal University of Uberlândia, Uberlândia, Brazil
[1]pedrobonnas@ufu.br, [2]tobias@ufu.br

Abstract. *In this work an identification procedure aiming to determine a reduced order model (ROM) of a linear time–invariant (LTI) aeroelastic model is presented. In order to present the details of the proposed technique, a rigid airfoil section considering only the pitch–plunge motion is studied in a fluid–structure interaction scheme using Computational Fluid Dynamics (CFD). The Identification methodology applied to generate the ROM is based on the use of orthogonal functions and their integration properties to transform the aeroelastic system differential equations of motion into a set of algebraic linear equations where the unknown parameters can be determined. The structural parameters of the linear mechanical system are initially known and built on COMSOL Multiphysics®. Based on the input and the output of the system, it is possible to determine the parameters of the aerodynamic loads applied by the CFD in order to develop the ROM. The identified flow–field model is then used to determine the system response for several airflow speeds, avoiding the systematic use of CFD, thus optimizing engineering projects.*

Keywords: *aeroelasticity, system identification, orthogonal functions, reduced order model.*

1. INTRODUCTION

With the subsequent development of computational fluid dynamics (CFD) technology, the science and practice of aeroelasticity have evolved into a new stage over the last decade. Aeroelasticity is the study field that is concerned with the couplings between structural mechanics and the physical principles of fluid dynamics, considering the aerodynamic, structural and inertial forces (Wright and Cooper, 2008). While CFD tools are quite powerful and provide significant insight regarding flow physics, relatively simple models of unsteady flows about wings and airfoils are quite complex to compute (Anderson and Wendt, 1995), which causes great effect on how aeroelastic analysis are performed due to the increase in computational cost (Silva, 2018).

In order to avoid excessive computing time encountered during unsteady aeroelasticity calculations, CFD-based reduced-order models (ROMs) have been developed and used (Kim *et al.*, 2005). Reduced order models are usually generated from system identification methods, which are procedures that can develop or improve a mathematical representation of a physical system based either on experimental or simulated data. For projects that the system response and initial conditions are available and the mathematical model of the mechanical structure is known, the identification procedure can be written as a classical inverse problem. System identification is a critical stage in aircraft development, analysis, and validation (Kukreja and Brenner, 2006).

In the last decade, many works have been dedicated to the identification of unsteady aerodynamic systems. Hall (1994) developed a general technique for constructing reduced order models of unsteady aerodynamic flows about two dimensional isolated airfoils, cascades of airfoils, and three-dimensional wings. After that, Hall *et al.* (1995) presented a new technique for computing unsteady flows about turbomachinery cascades. Florea and Hall (1998) also created a new approach for computing unsteady flows about isolated airfoils based in the dominant natural frequencies (eigenvalues) and mode shapes (eigenmodes) of unsteady fluid motion about the airfoil. Romanowski and Dowell (1996) extended the reduced order modelling technique to realistic computational mesh sizes.

In this work an identification procedure aiming to establish a linear time-invariant (LTI) aeroelastic airfoil system is presented. In order to present the details of the proposed technique, a linear airfoil considering only the pitch – plunge motion is studied. The methodology used is based on the use of orthogonal functions and their integration properties, which can transform the aeroelastic system differential equations of motion into a set of algebraic linear equations where the unknown parameters related to the aerodynamic loads can be determined.

The use of the orthogonal functions and its proprieties to solve inverse problems is widely found in the literature. Chen and Hsiao (1975) developed techniques for parameter identification using orthogonal functions. Steffen Jr and Rade (1991) developed this methodology on a multi-degree-of-freedom linear mechanical system. Then, Melo and Steffen Jr

(1993) validated experimentally the developed methodology for a three-degree-of-freedom mechanical system. Pacheco and Steffen Jr (2002) also implemented this methodology using various orthogonal functions.

The structural parameters of the linear mechanical system are initially known and implemented in COMSOL®. Then, a fluid – structure interaction is simulated with the application of computational fluid dynamics (CFD). Although the CFD has nonlinear characteristics, the aeroelastic system is conceived around a equilibrium position, which makes the model presents small displacements, making it possible to consider a linear behavior. The developed identification procedure is performed for a low order of degree-of-freedom system. For higher degree-of-freedom systems is recommended to establish the procedure considering the modal parameters identification, as observed in Morais *et al.* (2020). The biggest advantage of the identified model is its ability to determine the system response for several airflow speeds and conditions, avoiding the systematic use of the CFD, thus optimizing engineering projects.

2. METHODOLOGY

The proposed procedure for the identification of the aeroelastic system is organized according to three main steps. Primarily, the aeroelastic model is presented. Next, the proposed orthogonal function and its integration property are described. Finally, the identification procedure applied to the linear aeroelastic model is presented in detail.

2.1 Aeroelastic model

The aeroelastic model was built in COMSOL Multiphysics®. Figure 1 presents the structural model of the aeroelastic system, which is based in the cross section of a wing, represented by the NACA 0010 airfoil. The structural model of chord c and wingspan s (considered for mass calculations) has two degrees of freedom (h and θ) with a flexural rigidity k_h and torsional rigidity k_θ. The elastic axis is located at a distance e ahead the airfoil center of mass.

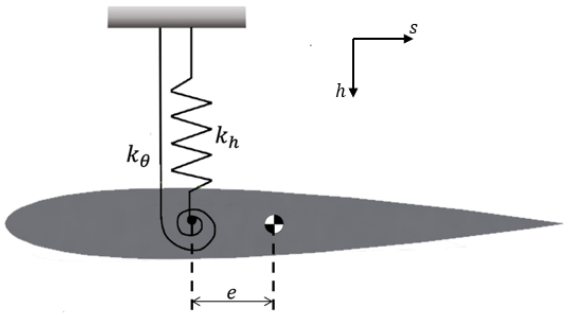

Figure 1. Structural representation of the aeroelastic system.

The aerodynamic model was defined as a turbulent stream in the s direction, conceived by the $k-\epsilon$ model. Various forms of the $k-\epsilon$ model have been in use for several decades, becoming the most used turbulent model for industrial applications (Spalding, 1974). For the fluid-structure interaction, the fully coupled FSI solver was used. This solver computes the couplings that appear at the limits between the fluid and the structure (fluid pressure and viscous forces). For the numerical solution, the Generalized Alpha method was used. The Generalized Alpha method is similar to the Backward Differentiation Formula method (BDF), but differs in its ability to control the degree of damping added by the solver, making the solution more accurate, but less numerically stable (Chung and Hulbert, 1993).

The values for the structural dynamic matrices were obtained with COMSOL®. These matrices can be verified by determining the differential equations of motion of the system using the Lagrange Equation, given by:

$$\frac{d}{dt}\left(\frac{\partial \mathcal{L}}{\partial \dot{q_j}}\right) - \frac{\partial \mathcal{L}}{\partial q_j} = Q_j \tag{1}$$

$$\mathcal{L} = T - V \tag{2}$$

where T is the kinetic energy, V is the potential energy, q_j are the generalized coordinates and Q_j are the generalized external forces, where j is the minimum coordinates number that represents the system ($j = 1, 2, 3, \dots$). The kinetic and potential energy of the structural system are given by Eq. (3) and Eq. (4), respectively.

$$T = \frac{1}{2} m \left(\dot{h}(t) + e\dot{\theta}(t)\right)^2 + \frac{1}{2} I \dot{\theta}(t)^2 \tag{3}$$

$$V = \frac{1}{2}k_h h(t)^2 + \frac{1}{2}k_\theta \theta(t)^2 \tag{4}$$

where m is the airfoil mass and I is the moment of inertia. Substituting Eq. (3) and Eq. (4) into Eq. (2) and Eq. (1) we obtain the equations of motion of the structural model:

$$\begin{bmatrix} m & me \\ me & I + me^2 \end{bmatrix} \begin{Bmatrix} \ddot{h}(t) \\ \ddot{\theta}(t) \end{Bmatrix} + \begin{bmatrix} k_h & 0 \\ 0 & k_\theta \end{bmatrix} \begin{Bmatrix} h(t) \\ \theta(t) \end{Bmatrix} = \begin{Bmatrix} -L(t) \\ \tau(t) \end{Bmatrix} \tag{5}$$

Equation (5) can be written as follows:

$$[M]\{\ddot{x}(t)\} + [K]\{x(t)\} = \{f(t)\} \tag{6}$$

where $[M]$ and $[K]$ are the structural mass and stiffness matrices, L is the vertical aerodynamic force at the center of pressure, τ is the moment caused by L in the elastic axis and $\{x(t)\}$ is the state vector. Applying the simplified unstable aerodynamics to the dynamic model in Eq. (6) it is possible to obtain the expression of the full aeroelastic equation of motion subjected to aerodynamics forces $\{f(t)\}$, given by:

$$[M]\{\ddot{x}(t)\} + \rho V[C_{aero}]\{\dot{x}(t)\} + [\rho V^2 K_{aero} + K]\{x(t)\} = \{f(t)\} \tag{7}$$

where $[C_{aero}]$ and $[K_{aero}]$ are the aerodynamic damping and aerodynamic stiffness matrices, ρ is the air density and V is the stream velocity. From the identification methodology, the main objective is to determine the aerodynamic damping $[C_{aero}]$ and the aerodynamic stiffness $[K_{aero}]$ added by the fluid – structure interaction.

2.2 The orthogonal function

Since the identification procedure is based on orthogonal functions, its definition is given by (Spiegel, 1976):

$$\int_a^b \varphi_m(t)\varphi_n(t)dt = K, \text{where} \begin{cases} K = 0 \Rightarrow m \neq n \\ K \neq 0 \Rightarrow m = n \end{cases} \tag{8}$$

where a set of real functions $\varphi_k(t)$ $(k = 1, 2, 3, \dots)$ is said to be orthogonal in the interval $[a, b]$ if Eq. (8) is satisfied. Equation (9) presents an important integration property of orthogonal functions that holds for a set of r functions in the interval $[0, t]$.

$$\int_0^t \underbrace{\dots}_{\text{n times}} \int_0^t \{\phi(t)\}(dt^n) \cong [P]^n \phi(t) \tag{9}$$

where $\{\phi(t)\}$ is the finite group of the orthogonal series and $[P]$ is a square matrix of order r with constant elements, called operational integration matrix. For the identification procedure developed, the Fourier series basis vector $\{\phi(t)\}$ was used, given by (Spiegel, 1976):

$$\{\phi(t)\} = \{\phi_0(t)\ \phi_1(t)\ \dots\ \phi_s(t)\ \ \phi_1^*(t)\ \dots\ \phi_s^*(t)\}^T \tag{10}$$

where:

$$\phi_n(t) = \cos\left(\frac{2n\pi t}{T}\right)\ n = 0, 1, ..., s \tag{11}$$

$$\phi_n^*(t) = \sin\left(\frac{2n\pi t}{T}\right)\ n = 1, ..., s \tag{12}$$

The operational integration matrix for the Fourier series basis for a time period interval of $[0, T]$ is given by:

$$[P] = \begin{bmatrix} \frac{T}{2} & 0 & 0 & \cdots & 0 & \frac{-T}{\pi} & \frac{-T}{2\pi} & \cdots & \frac{-T}{s\pi} \\ 0 & 0 & 0 & \cdots & 0 & \frac{T}{2\pi} & 0 & \cdots & 0 \\ 0 & 0 & 0 & \cdots & 0 & 0 & \frac{T}{4\pi} & \cdots & 0 \\ \vdots & \vdots & \vdots & \ddots & \vdots & \vdots & \vdots & \ddots & \vdots \\ 0 & 0 & 0 & \cdots & 0 & 0 & 0 & \cdots & \frac{T}{2s\pi} \\ \frac{T}{2\pi} & \frac{-T}{2\pi} & 0 & \cdots & 0 & 0 & 0 & \cdots & 0 \\ \frac{T}{4\pi} & 0 & \frac{-T}{4\pi} & \cdots & 0 & 0 & 0 & \cdots & 0 \\ \vdots & \vdots & \vdots & \ddots & \vdots & \vdots & \vdots & \ddots & \vdots \\ \frac{T}{2s\pi} & 0 & 0 & \cdots & \frac{T}{2s\pi} & 0 & 0 & \cdots & 0 \end{bmatrix} \tag{13}$$

2.3 The identification procedure

The main idea of the identification procedure is to transform the aeroelastic system equations of motion (Eq. 7) into a linear equation, where, $[C_{aero}]$ and $[K_{aero}]$ can be determined, thus identifying the aerodynamics loads applied by the CFD. First, $\{x(t)\}$ and $\{f(t)\}$ are expanded into series of orthogonal functions with r terms:

$$\{x(t)\} = [X]\{\phi(t)\} \tag{14}$$

$$\{f(t)\} = [F]\{\phi(t)\} \tag{15}$$

where $[X]$ is the $(n \times r)$ matrix of the expansion coefficients of $\{x(t)\}$ and $[F]$ is the $(n \times r)$ matrix of the expansion coefficients of $\{f(t)\}$. After the expansion, we substitute Eq. (14) and Eq. (15) into Eq. (7) and integrate twice on the interval $[0, t]$:

$$\begin{aligned}[M]([X]\{\phi(t)\} - \{x(0)\} - \{\dot{x}(0)\}t) + \rho V[C_{aero}]\left(\int_0^t [X]\{\phi(t)\}dt - \{x(0)\}t\right) \\ + \rho V^2[K_{aero}]\left(\int_0^t\int_0^t [X]\{\phi(t)\}dt^2\right) + [K]\left(\int_0^t\int_0^t [X]\{\phi(t)\}dt^2\right) = \int_0^t\int_0^t [F]\{\phi(t)\}dt^2\end{aligned} \tag{16}$$

It's observed that the first function of the orthogonal series is equal to 1 for any instant t. Thus, we can write:

$$\{e\}^T\{\phi(t)\} = 1 \tag{17}$$

where $\{e\}^T = \{1 \quad 0 \quad ... \ 0\}$. Integrating Eq. (17) on the interval $[0, t]$ and applying the integration property given by Eq. (9):

$$t = \{e\}^T[P]\{\phi(t)\} \tag{18}$$

Substituting Eq. (18) and Eq. (17) into Eq. (16) and applying the integration property given by Eq. (9), we obtain:

$$\begin{bmatrix} M & C & K & -F & -Mx_0 & -M\dot{x}_0 - Cx_0 \end{bmatrix} \begin{bmatrix} X \\ XP \\ XPP \\ PP \\ e^T \\ e^T P \end{bmatrix} = \begin{bmatrix} \rho V C_{aero} & \rho V^2 K_{aero} & -C_{aero} x_0 \end{bmatrix} \begin{bmatrix} XP \\ XPP \\ e^T P \end{bmatrix} \quad (19)$$

Equation (19) can be written as follows:

$$HJ = H_{aero} J_a \quad (20)$$

As the matrices H, J and J_a are known, we can determine H_{aero}, thus finding $[C_{aero}]$ and $[K_{aero}]$.

3. SIMULATION AND RESULTS

The simulation of the CFD-based unsteady aerodynamic system was performed considering a steady flow with a free stream velocity V of 40 m/s. The parameters used to simulate the system are presented in Table 1.

Table 1. Structural and aerodynamic parameters used to simulate the aeroelastic response.

Parameter	**Value**
c [m]	1
s [m]	1
Material Density ρ [kg/m^3]	2.000
k_h [N/m]	30.000
k_θ [N/rad]	6666.67
Bending Nat. Freq. f_{n1} [Hz]	2.31
Torsional Nat. Freq. f_{n2} [Hz]	4.85
e [m]	0.0845
Air Density ρ_∞ [kg/m^3] (1)	1.225
Air Dynamic Viscosity μ_∞ [Pa.s] (1)	1.802 $\times 10^{-5}$

(1) Measured at 15 ^{o}C.

A fundamental analysis previous to the CFD simulation is the study of the candidates for the input functions for the structural modes excitation. System identification techniques dictates that the nature of the input functions used to excite the system must be properly defined (Silva, 2008). Section 3.1 presents a few candidates for the input functions.

3.1 Input functions for simultaneous excitation

In order to determine what kind of input functions we can use for the excitation of the structural modes of the aeroelastic system we have to consider some important requirements. Considering that the goal is the simultaneous excitation of a two-input-output system, an important point to keep in mind is that the input functions for each structural mode must

be different, in some sense, from each other (Silva, 2008). If the excitation inputs are the correlated and they are applied simultaneously, it becomes practically impossible for any system identification algorithm to relate the effects of one input on a given output, which is a fundamental condition towards the development of reduced order models (Silva, 2008). Thus, the study of the input functions comes down to the analysis of how different these functions should be and how can we quantify this level of "difference" between each input function.

Silva (2008) focused on some specific orthogonal functions as candidates for input functions in his identification work, knowing that orthogonality (linear independence) is the most precise mathematical method for guaranteeing the difference between signals. Silva (2008) presents three input functions as candidates: block pulse, Haar and Walsh, which are modified step input functions. This class of functions are considered optimal input functions because in addition to being as different as mathematically possible, they excite a broad frequency bandwidth, guaranteeing multiple modes excitation.

Although the modified step functions presented by Silva (2008) are considered to be optimal input functions, they are not ideal for the identification procedure developed in this work. As shown in Section 2.2, the Fourier series basis vector was used. Since the signal of the input function is expanded (Eq. 15), the Gibbs phenomenon becomes considerable, arising substantial errors in the identification procedure. The Gibbs phenomenon is characterized by distortions in the extremities of the graphs, as presented in Figure 2.

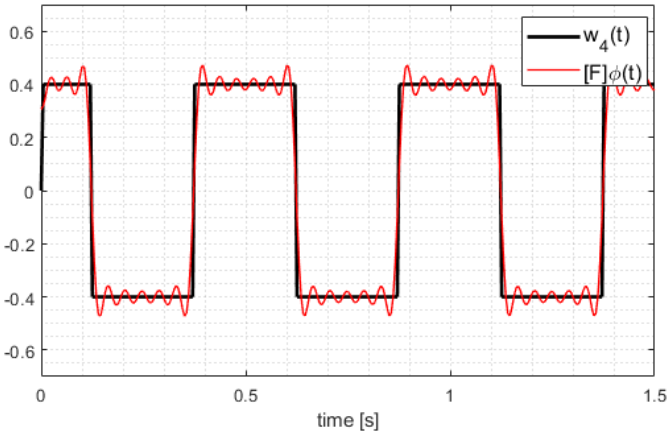

Figure 2. Gibbs phenomenon in the Walsh function expansion, $r = 241$.

Therefore, in order to select the correct input function for the identification procedure of this work, the following must be considered. First, one must use different input functions for each structural modal excitation. Second, this functions must be expandable by the Fourier basis in order to avoid greater errors related to the Gibbs phenomenon. Third, these functions must excite a broad frequency bandwidth, in order to guarantee multiple modes excitation, thus making the reduced order model representative. Two types of signals that fulfil the mentioned requirements were studied: random signals and filtered random signals.

Random signals have been widely used in identifications procedures of mechanical systems as input functions by many authors in the last decade. Unfortunately, as shown in Figure 3, random signals have sharp and rapidly changing values, causing the CFD to demand a very large number of subiterations in order to achieve a moderate rate of convergence especially in the critical low-frequency range and, hence, a very long computing time overall, not becoming viable for CFD model reduction in general (Kim *et al.*, 2005).

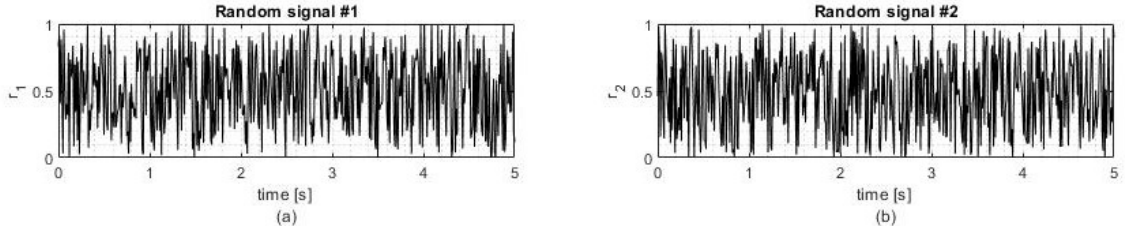

Figure 3. Two random signals generated with MATLAB®.

In order to add smooth inputs to CFD, one can filter a random signal through a low-frequency filter, allowing better convergence in the CFD solutions (Kim *et al.*, 2005). This type of signal (labeled Filtered Random Signal - FRS) was the selected input function for the simulation. Note that r_i represents a random signal which is identical to a sequence of arbitrary numbers and r_{fi} is identical to a sequence of filtered random numbers.

Based on the theory of ergodicity (Papoulis and Saunders, 1989), statistical independence could be fortified by using longer signals and sampling the response for a longer period of time. Since sampling the response for a long period of time is impracticable with CFD, statistical independence must be achieved with a different approach.

In order to maintain a distinct difference between input signals, each signal must excite a specific frequency bandwidth, that is, there must not be overlapping excited frequency input bands. Thus, the input signal related to the first structural mode must act in a specific interval near the first natural frequency f_{n1} and the input signal related to the second structural mode must act in another specific interval near the second natural frequency f_{n2}. Such frequency bandwidths separation can be achieved by applying a low-pass filter to r_1 and a band-pass filter to r_2, thus guaranteeing independence of the input signals. The parameters used to filter each signal are stated in Table 2. Figure 4 presents both r_{f1} and r_{f2} filtered signals.

Table 2. Filter parameters used to filter r_1 and r_2.

Low-pass filter parameters	**Value**
Cutoff frequency f_c	2.6 Hz
Band-pass filter parameters	**Value**
Low frequency f_L	4.5 Hz
High frequency f_H	6.0 Hz

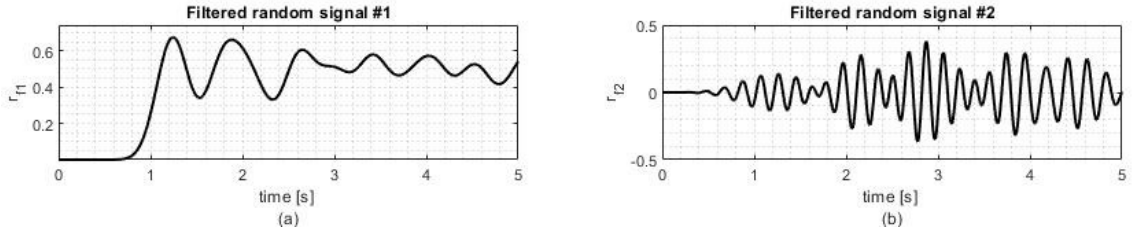

Figure 4. Filtered random signals r_{f1} and r_{f2}.

The input functions used in the simulation are defined in terms of force and momentum at the elastic axis, given by:

$$\left\{f(t)\right\} = \begin{Bmatrix} 100\ r_{f1} \\ -300\ r_{f2} \end{Bmatrix} \begin{matrix} \text{[N]} \\ \text{[N.m]} \end{matrix} \tag{21}$$

3.2 Results

The responses of both structural modes were monitored from the acquisition of the elastic center vertical displacement at the h axis and the elastic center rotation about the z axis (pointing into the paper). From the methodology presented in Section 2, a aeroelastic system identification algorithm was written in MATLAB®. Figure 5 presents a comparison of the dynamic aeroelastic response of the first structural mode from the CFD aeroelastic simulation performed in COMSOL® with the ROM aeroelastic solution at a stream velocity of 40 m/s. Figure 6 presents a comparison of the dynamic aeroelastic response of the second structural mode from the CFD aeroelastic simulation performed in COMSOL® with the ROM aeroelastic solution at the same condition. Figure 7 presents the V-g-f plots and Figure 8 presents the aeroelastic root locus plot, both varying with the stream velocity from 0 to 50 m/s. Each point in Figure 8 represents the aeroelastic roots of the system at a specific stream velocity, with an increment of 1 m/s for each following point. Figure 9 presents a close-up version of the root locus plot for the first structural mode. This root locus indicates a flutter mechanism dominated by the first mode approximately at 48 m/s while the second modes remains stable.

4. CONCLUSION

As can be seen in Figures 5 and 6, the generated results indicates an outstanding level of correlation between the CFD aeroelastic solution and the ROM solutions, indicating good confidence in the ROM. Therefore, we can conclude that the proposed methodology demonstrates to be suitable for the identification of linear aeroelastic systems, thus making possible to generate aeroelastic responses for several airflow speeds at the same simulated subsonic region without the systematic use of CFD. Furthermore, the developed ROM methodology has the ability to rapidly generate aeroelastic analysis presented in the form of velocity-damping-frequency (V-g-f) plots and root locus plots that exposes the aeroelastic mechanisms occurring at the specified flight condition.

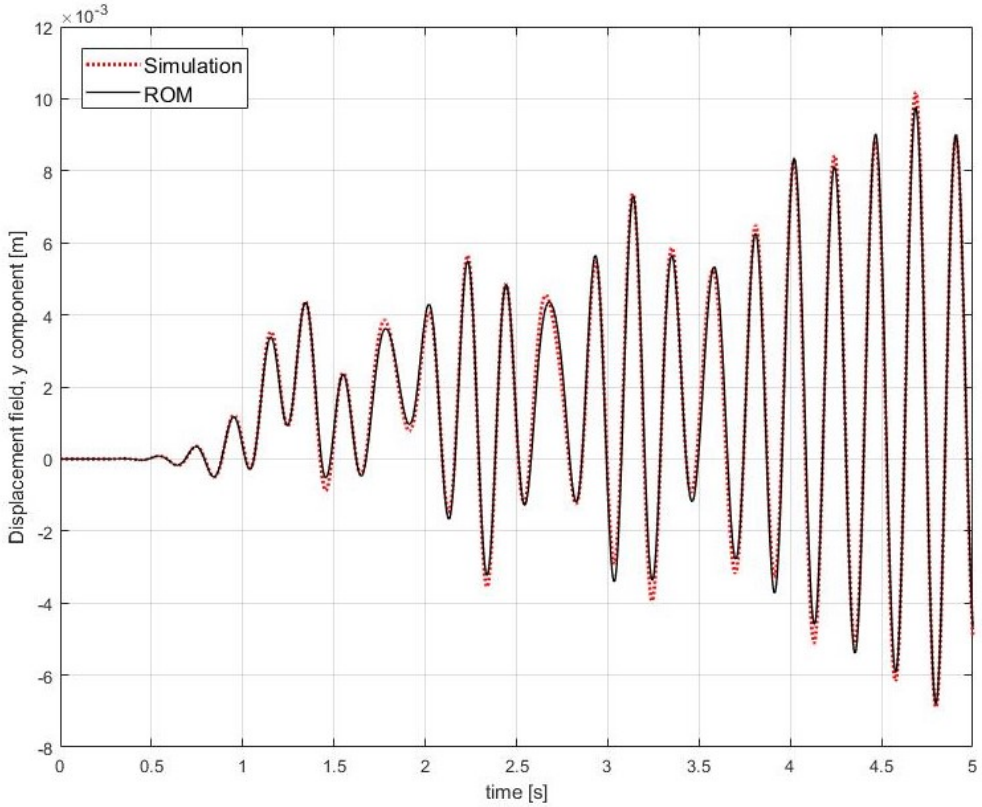

Figure 5. Comparison of the CFD aeroelastic response and the ROM aeroelastic response for the first mode at $V = 40$ m/s, $r = 121$.

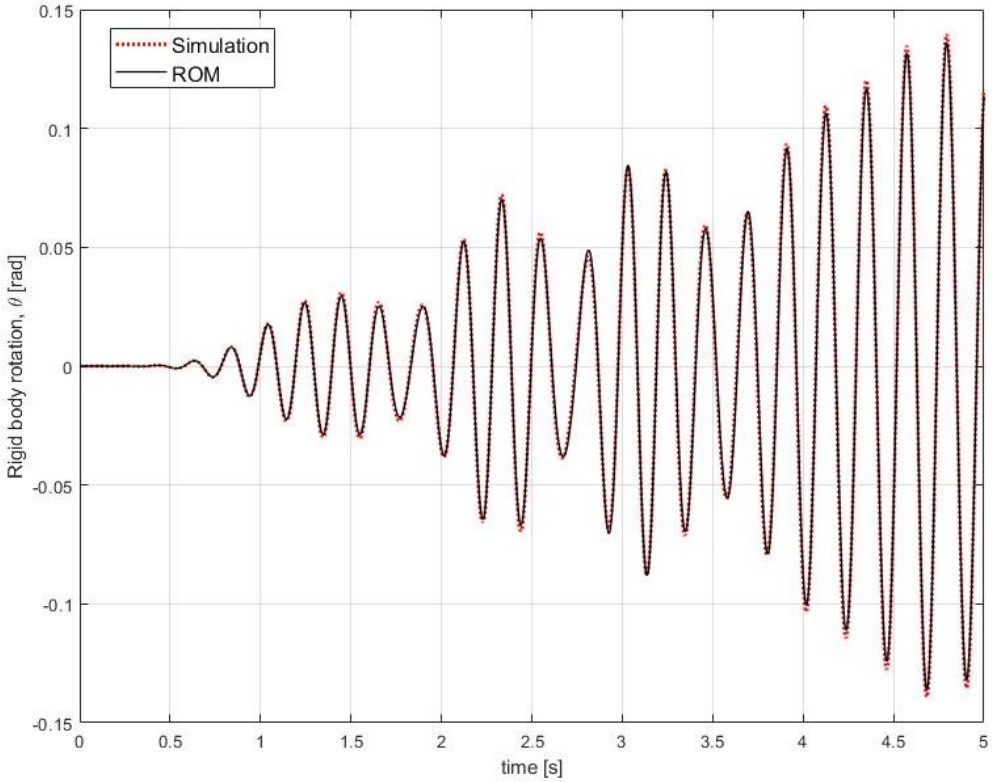

Figure 6. Comparison of the CFD aeroelastic response and the ROM aeroelastic response for the second mode at $V = 40$ m/s, $r = 121$.

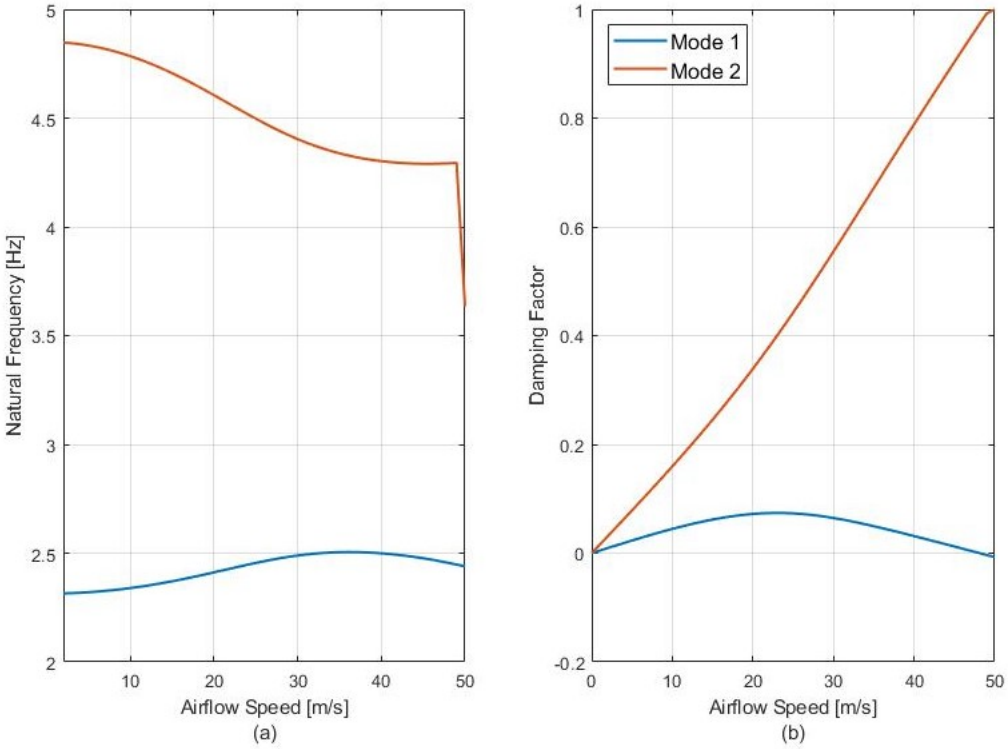

Figure 7. Velocity-damping-frequency plots generated from the ROM.

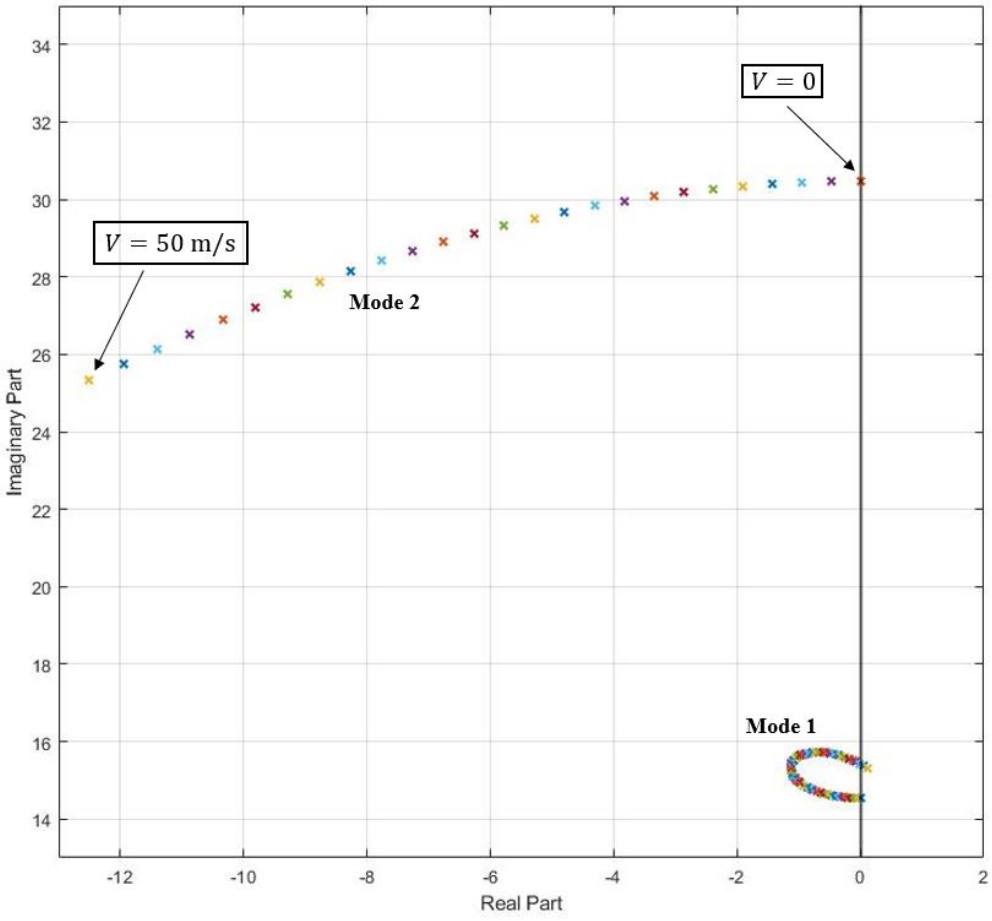

Figure 8. Root locus plot generated from the ROM with each point indicating a increment of 1m/s in the stream velocity.

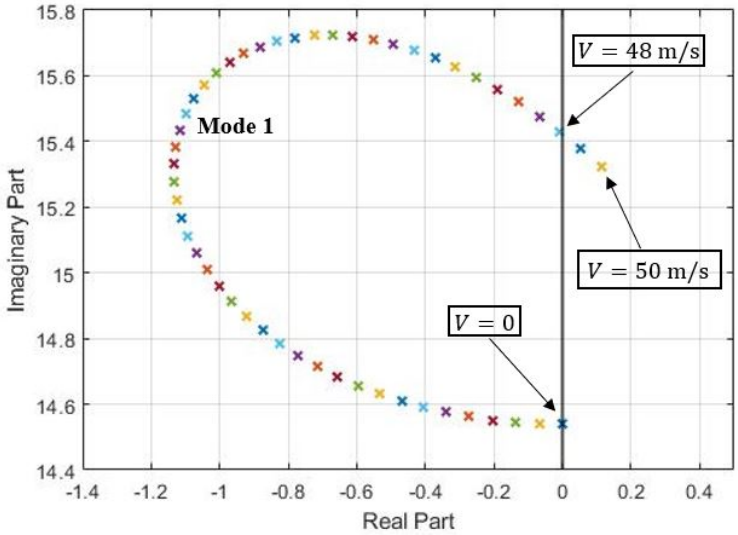

Figure 9. Close-up version of the root locus plot for the first structural mode.

5. REFERENCES

Anderson, J.D. and Wendt, J., 1995. *Computational Fluid Dynamics*, Vol. 206. Springer.

Chen, C. and Hsiao, C., 1975. "Time-domain synthesis via walsh functions". In *Proceedings of the Institution of Electrical Engineers*. IET, Vol. 122, pp. 565–570.

Chung, J. and Hulbert, G., 1993. "A time integration algorithm for structural dynamics with improved numerical dissipation: the generalized-α method".

Florea, R. and Hall, K.C., 1998. "Eigenmode analysis of unsteady flows about airfoils". *Journal of Computational Physics*, Vol. 147, No. 2, pp. 568–593.

Hall, K., Florea, R. and Lanzkron, P., 1995. "A reduced order model of unsteady flows in turbomachinery".

Hall, K.C., 1994. "Eigenanalysis of unsteady flows about airfoils, cascades, and wings". *AIAA journal*, Vol. 32, No. 12, pp. 2426–2432.

Kim, T., Hong, M., Bhatia, K.G. and SenGupta, G., 2005. "Aeroelastic model reduction for affordable computational fluid dynamics-based flutter analysis". *AIAA journal*, Vol. 43, No. 12, pp. 2487–2495.

Kukreja, S.L. and Brenner, M.J., 2006. "Nonlinear aeroelastic system identification with application to experimental data". *Journal of guidance, control, and dynamics*, Vol. 29, No. 2, pp. 374–381.

Melo, G. and Steffen Jr, V., 1993. "Mechanical systems identification through fourier series time-domain technique". *Journal of the Brazilian Society of Mechanical Sciences*, Vol. 15, No. 2, pp. 124–135.

Morais, T.S., de Souza Leão, L., Ap Cavalini Jr, A. and Steffen Jr, V., 2020. "Rotating machinery health evaluation by modal force identification". *Inverse Problems in Science and Engineering*, Vol. 28, No. 5, pp. 695–715.

Pacheco, R. and Steffen Jr, V., 2002. "Using orthogonal functions for identification and sensitivity analysis of mechanical systems". *Journal of Vibration and Control*, Vol. 8, No. 7, pp. 993–1021.

Papoulis, A. and Saunders, H., 1989. "Probability, random variables and stochastic processes".

Romanowski, M. and Dowell, E., 1996. "Reduced order euler equations for unsteady aerodynamic flows-numerical techniques". In *34th Aerospace Sciences Meeting and Exhibit*. p. 528.

Silva, W.A., 2008. "Simultaneous excitation of multiple-input/multiple-output cfd-based unsteady aerodynamic systems". *Journal of Aircraft*, Vol. 45, No. 4, pp. 1267–1274.

Silva, W.A., 2018. "Aerom: Nasa's unsteady aerodynamic and aeroelastic reduced-order modeling software". *Aerospace*, Vol. 5, No. 2, p. 41.

Spalding, D., 1974. "The numerical computation of turbulent flow". *Comp. Methods Appl. Mech. Eng.*, Vol. 3.

Spiegel, M.R., 1976. *Analise de FOURIER.* McGraw-Hill.

Steffen Jr, V. and Rade, D., 1991. "An identification method of multi-degree-of-freedom system based on fourier series". *The International Journal of Analytical and Experimental Modal Analysis*, Vol. 6, No. 4, pp. 271–278.

Wright, J.R. and Cooper, J.E., 2008. *Introduction to aircraft aeroelasticity and loads*, Vol. 20. John Wiley & Sons.

6. RESPONSIBILITY NOTICE

The authors are solely responsible for the printed material included in this paper.